Accurate Analysis of Tapered Planar Transmission Lines for Microwave Integrated Circuits

D. MIRSHEKAR-SYAHKAL AND J. BRIAN DAVIES, MEMBER, IEEE

Abstract—**A broad class of nonuniform transmission lines is analyzed through the method of coupled modes accompanied by the spectral domain solution of uniform lines. This combination offers efficient computation of the coupling coefficients. Small coupling allows the rigorous field theory of the spectral domain approach to give explicitly the scattering matrix of the taper. Several structures, including microstrip to coplanar waveguide taper and waveguide to fin-line taper, are successfully analyzed. The computed values of reflection coefficients are compared with the values derived by a simple impedance method and with the measured values. Results from the experimentally investigated tapers show that the theory is in good agreement.**

I. Introduction

SO FAR, no accurate analysis has been given for nonuniform planar transmission lines, as used in MIC. Although in one case, for a microstrip taper [1], the author approached the problem via the generalized telegraphist's equations [2], it is very common to investigate these types of transitions through a simple impedance method [3]. However, since the notion of characteristic impedance in planar transmission lines is contentious, (due to the mixed dielectric loading, e.g., [4], [5]), the impedance method cannot be regarded as a reliable technique. In fact, the major complexity for efficient and accurate analysis of uniform or nonuniform planar structures here lies in the necessary treatment of hybrid modes to which there is no closed-form solution.

Access to fast and accurate analysis of uniform planar transmission lines by the spectral domain method [6] now allows the three dimensional problems of tapered planar transmission lines to be formulated through the powerful coupled-mode theory [7], [8]. A combination of the coupled-mode technique and the spectral domain approach is adequately fast from the computing standpoint. Furthermore, the analysis is general, so that, unlike the treatment given in [1] for microstrip tapers, it can be applied to a broad class of planar transmission line tapers. The high efficiency in this new approach is directly associated with the existence of the spectral domain technique, giving the opportunity of conversion of involved integrals into easily computed series.

Manuscript received June 12, 1980; revised September 30, 1980.

The authors are with the Department of Electronic and Electrical Engineering, University College, London WCIE J7E, England.

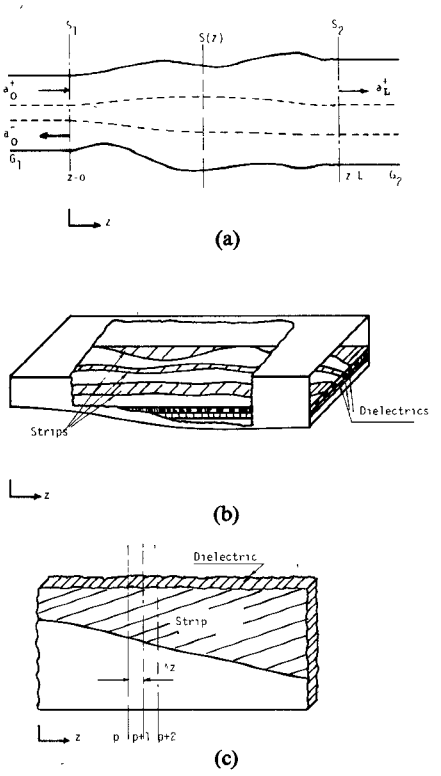

Fig. 1. (a) A general transition. (b) A general planar taper. (c) A portion of the planar taper of Fig. 1(b).

II. Theory

Let the uniform guide G_1 be connected to another uniform guide G_2 through a gentle transition (Fig. 1(a)). It is assumed that the first derivatives of all electrical and mechanical parameters with respect to z at the joining planes S_1 and S_2 vanish. Furthermore, the conductors are perfect and dielectric media are assumed homogeneous, isotropic, and lossless. The system is also nonradiating which could always be achieved by introducing a perfect conductor enclosure.

Suppose that the transverse field components of normal modes of propagation for a uniform guide with cross section identical to $S(z)$ be represented by $\boldsymbol{e}_t(x, y, \beta_\gamma)$ and $\boldsymbol{h}_t(x, y, \beta_\gamma)$. The normal modes satisfy Maxwell's equations, and, in view of appropriate normalization, obey the

0018-9480/81/0200-0123$00.75 ©1981 IEEE

following orthogonality relation [9]:

$$\int_{S(z)} \boldsymbol{e}_t(x,y,\beta_\gamma)\times\boldsymbol{h}_t^*(x,y,\beta_\mu)\cdot\boldsymbol{a}_z\,ds=\delta_{\gamma\mu} \tag{1}$$

where $\delta_{\mu\gamma}$ is the Kronecker delta. As the uniform guide changes its characteristic gradually in the direction of propagation in accordance with the transition, the normal modes no longer are a solution of Maxwell's equations. Yet they can be considered as a complete set of basis functions to approximate the fields at any arbitrary cross section of the taper. Thus, the following field expansions in terms of normal fields are valid:

$$\boldsymbol{E}_t=\sum_\gamma (a_\gamma^+ + a_\gamma^-)\boldsymbol{e}_t(x,y,\beta_\gamma(z)) \tag{2}$$

$$\boldsymbol{H}_t=\sum_\gamma (a_\gamma^+ - a_\gamma^-)\boldsymbol{h}_t(x,y,\beta_\gamma(z)). \tag{3}$$

Substituting (2) and (3) in Maxwell's equations and noting the orthogonality relation (1), results in coupled-mode equations given by [7], [10]:

$$\frac{da_\mu^\mp}{dz}\mp j\beta_\mu(z)a_\mu^\mp=\pm\frac{1}{2}\sum_\gamma a_\gamma^+\left(K_{\mu,\gamma}\mp\tilde{K}_{\gamma,\mu}\right)\mp\frac{1}{2}\sum_\gamma a_\gamma^-\left(K_{\mu,\gamma}\pm\tilde{K}_{\gamma,\mu}\right) \tag{4}$$

where

$$K_{\mu,\gamma}=\int_{S(z)}\boldsymbol{e}_t^*(x,y,\beta_\mu(z))\times\frac{\partial\boldsymbol{h}_t(x,y,\beta_\gamma(z))}{\partial z}\cdot\boldsymbol{a}_z\,ds \tag{5}$$

$$\tilde{K}_{\gamma,\mu}=\int_{S(z)}\frac{\partial\boldsymbol{e}_t(x,y,\beta_\gamma(z))}{\partial z}\times\boldsymbol{h}_t^*(x,y,\beta_\mu(z))\cdot\boldsymbol{a}_z\,ds. \tag{6}$$

The above coupled differential equations (4) are valid as long as there is gradual change in the direction of propagation. However, for rapidly varying taper (not being considered in this work), one might analyze the problem via the more complicated procedure given by Stevenson [8].

Since we are concerned with one forward traveling wave and one backward traveling wave with identical phase constant $\beta(z)$, (4) is reduced to the following form if the other modes are neglected:

$$\frac{da^+}{dz}+j\beta(z)a^+=0 \tag{7}$$

$$\frac{da^-}{dz}-j\beta(z)a^-=C(z)a^+ \tag{8}$$

where

$$C(z)=\frac{1}{2}(K-\tilde{K}). \tag{9}$$

In equations (7), (8), and (9), subscript 1 representing the fundamental mode has been dropped. In (7), it is also assumed that coupling from backward mode to forward mode is negligible, which is true for gradual transitions, [11], [12]. The coupling is, of course, reciprocal, but for excitation in the a^+ mode, (7) and (8) give the leading terms in the overall scattering matrix.

Differential equations (7) and (8) have closed-form solutions. Assuming that the uniform guide G_2 in Fig. 1(a) extends to infinity, the following expressions are immediately derived:

$$a^+=a_0^+\exp\left(-j\int_0^z\beta(\zeta)\,d\zeta\right) \tag{10}$$

$$a^-=-a_0^+\int_0^L C(z)\exp\left(-j2\int_0^z\beta(\zeta)\,d\zeta\right)dz \tag{11}$$

where a_0^- denotes the reflected wave amplitude at S_1 plane, while a_0^+ and L represent the amplitude of incident wave and the length of transition, respectively. From (11), the reflection coefficient is given by

$$R=-\int_0^L C(z)\exp\left(-j2\int_0^z\beta(\zeta)\,d\zeta\right)dz. \tag{12}$$

Considering the impedance technique for taper analysis [3], an expression for reflection coefficient of a gradual transition is as follows:

$$\Gamma=-\int_0^L\rho(z)\exp\left(-2j\int_0^z\beta(\zeta)\,d\zeta\right)dz \tag{13}$$

where

$$\rho(z)=-\frac{1}{2}\frac{d}{dz}\ln\bar{Z}(z) \tag{14}$$

and $\bar{Z}(z)$ is normalized impedance.

Comparison of (12) and (13) reveals that the only difference between these two expressions is in the exchange of functions $C(z)$ and $\rho(z)$. This means that any difference between $C(z)$ and $\rho(z)$ leads to different reflection coefficients. It is emphasized again that the value of characteristic impedance is contentious for planar transmission lines, so that reflection coefficients computed through (13) do not appear to be unique. Also, the impedance method is usually implemented to single-mode operated transitions, while the coupled-mode approach has no restriction as such and can be applied to multimode conditions as well. Nonetheless (13), under certain conditions, as concluded later, could be regarded as a possible approximation to (12).

Now consider Fig. 1(b), showing a general planar transition. We proceed with the assumptions that the sides and the top conductor of the shield remain constant throughout the transition region (Fig. 1(b)). However, these restrictions do not limit the generality of solution and only ease the labor involved in achieving the analytical expression of $C(z)$.

For any arbitrary cross section along the transition region of Fig. 1(b), the transverse fields of normal modes can be obtained through the spectral domain technique [5], [6], [13]. As an example, these fields for the first dielectric region in their transformed form are given by

$$\tilde{E}_{x1},\tilde{H}_{y1}=\left(\tilde{e}_{x1},\tilde{h}_{y1}\right)\mathrm{Sh}(\gamma_{1n}y)/\mathrm{Sh}(\gamma_{1n}h_1) \tag{15}$$

$$\tilde{H}_{x1},\tilde{E}_{y1}=j\left(\tilde{h}_{x1},\tilde{e}_{y1}\right)\mathrm{Ch}(\gamma_{1n}y)/\mathrm{Ch}(\gamma_{1n}h_1) \tag{16}$$

where $\tilde{e}_{x1}$, $\tilde{h}_{y1}$, $\tilde{h}_{x1}$, $\tilde{e}_{y1}$, and γ_{1n} are functions of z and are

available in detail in [5]. h_1 represents the thickness of the mentioned dielectric region and may vary with z. Considering (1), equations (15) and (16) must be normalized before they are substituted in any other expression.

Assuming (15) and (16) are normalized, $C(z)$ is obtained once the z-derivatives of the transverse field components are known. For instance, from (15), the z-derivative of the Fourier transform of H_{y1} is written as follows:

$$\frac{\partial}{\partial z}\tilde{H}_{y1}=A_{y1}\frac{\mathrm{Sh}(\gamma_{1n}y)}{\mathrm{Sh}(\gamma_{1n}h_1)}+B_{y1}y\frac{\mathrm{Ch}(\gamma_{1n}y)}{\mathrm{Ch}(\gamma_{1n}h_1)} \tag{17}$$

where for example

$$A_{y1}=\frac{\partial}{\partial z}\tilde{h}_{y1}-\left(\gamma_{1n}\frac{\partial}{\partial z}h_1+h_1\frac{\partial}{\partial z}\gamma_{1n}\right)\tilde{h}_{y1}\coth(\gamma_{1n}h_1). \tag{18}$$

Very similar expressions to those given above for the first dielectric medium can be obtained for the other dielectric regions as well.

Having substituted appropriate fields and their derivatives in (9), $C(z)$ for a transition with F layers is given by

$$C(z)=\frac{1}{2}\sum_{i=1}^{F}\left(k_i-\tilde{k}_i\right) \tag{19}$$

where

$$k_i=a\sum_n\int_{h_{i-1}}^{h_i}\left(\tilde{E}_{xi}\frac{\partial}{\partial z}\tilde{H}^*_{yi}-\tilde{E}_{yi}\frac{\partial}{\partial z}\tilde{H}^*_{xi}\right)dy \tag{20}$$

$$\tilde{k}_i=a\sum_n\int_{h_{i-1}}^{h_i}\left(\tilde{H}_{yi}\frac{\partial}{\partial z}\tilde{E}^*_{xi}-\tilde{H}_{xi}\frac{\partial}{\partial z}\tilde{E}^*_{yi}\right)dy \tag{21}$$

where h_i in (20) and (21), like h_1 in (15) and (16), denotes the thickness of the ith substrate and $2a$ represents the transition width. From (15) to (18) it is concluded that the integrals involved in k_i and $\tilde{k}_i$ have closed-form solutions. Thereby, $C(z)$ is reduced to a simple series which can be truncated and computed very efficiently. In fact, experience shows that most of the computation time is consumed in finding the eigenvalues of normal modes, and calculation of $C(z)$ is not, itself, a time consuming process.

The only difficulty in computation of $C(z)$ arises from the fact that parameters such as $\tilde{h}_{y1}$ and γ_{1n} in (18) are not analytically differentiable. To overcome this problem, the taper length L is equally divided into M subsections with planes normal to z. Thus, we can approximate as (Fig. 1(c))

$$\frac{\partial\tilde{h}_{yi}}{\partial z}\simeq\frac{\tilde{h}^{p+1}_{yi}-\tilde{h}^{p}_{yi}}{\Delta z} \tag{22}$$

where $\Delta z=L/M$ and p and $p+1$ denote the two consecutive arbitrary cross sections. Approximation (22) will introduce some central difference errors in the value of $C(z)$, especially at the ends of the taper where, according to an earlier assumption, $C(z)$ has to vanish. By increasing M, this error has proved to have negligible effect on the overall reflection coefficient. All the above formulations are embedded in modified versions of the authors' computer programs [14] and applied to various tapers. Two of the more interesting transitions are examined as follows.

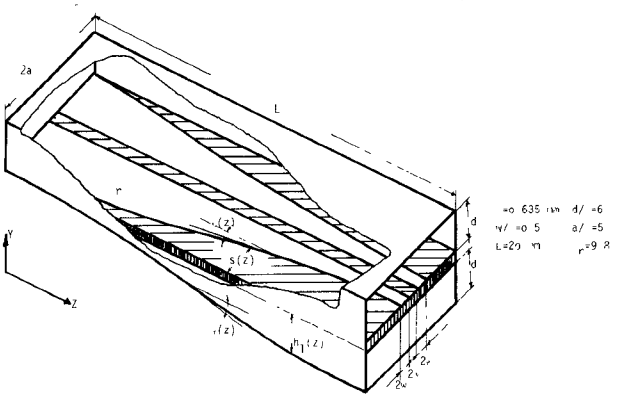

Fig. 2. Microstrip to coplanar waveguide taper.

III. Applications

A. Microstrip to Coplanar Waveguide Taper

Since coplanar waveguides have several advantages over the ordinary microstrips [15], a transition connecting these two lines would be of importance. This transition can be achieved by tapering the ground planes of both structures, Fig. 2. It is interesting to notice that the analysis of this taper via the impedance technique (13), would be almost impossible due to different definitions for the characteristic impedance given in the literature. For this transition, the bottom conductor and strip profiles are considered to be as follows:

$$h_1(z)=d\sin^2\frac{\pi z}{2L}$$

$$S(z)=(a-3w)\sin^2\frac{\pi z}{2L} \tag{23}$$

where a, w, d, and L are clearly shown in Fig. 2. The above profiles (23) satisfy the requirements both of vanishing $C(z)$ at either end of the taper and of smooth variation of geometry along the transition region. To find $C(z)$, transverse components of the normal modes in the Fourier domain, (i.e., 15 and 16) are computed in a way described in [5], [6]. It is found that the 5th-order solution is adequately accurate, (i.e., $P=Q=5$ in the notation of [13]), while the number of subsections M may be as high as 40.

For $M=20$, the values of $C(z)$ and $\rho(z)$ at 7.2 GHz have been plotted in Fig. 3. This comparison reveals the possible error present in the reflection coefficient evaluated through the impedance method. However, the same comparison at low frequency (1 GHz) showed that $C(z)$ and $\rho(z)$ are almost equal and so the choice between impedance and coupled wave approach does not alter the overall reflection coefficient substantially. It should be added that the characteristic impedance used in calculation $\rho(z)$ is defined through a voltage–power relation in which the voltage is defined from the center strip to the side wall in microstrip, or, to the neighboring strip acting as ground plane in the rest of the transition [5].

The return losses observed from each end of the transi-

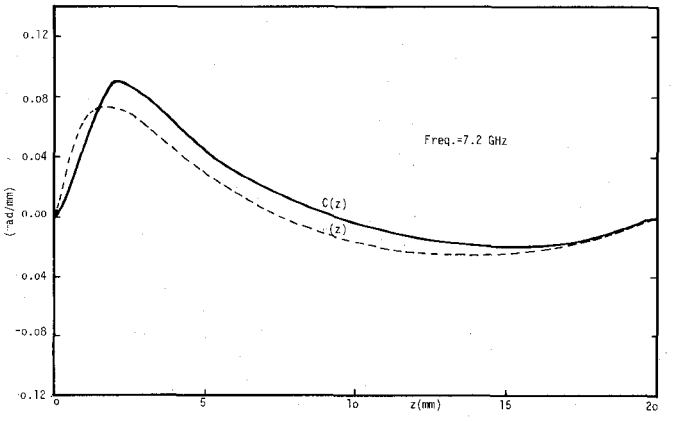

Fig. 3. Comparison of $\rho(z)$ and $C(z)$ along the transition length of Fig. 2.

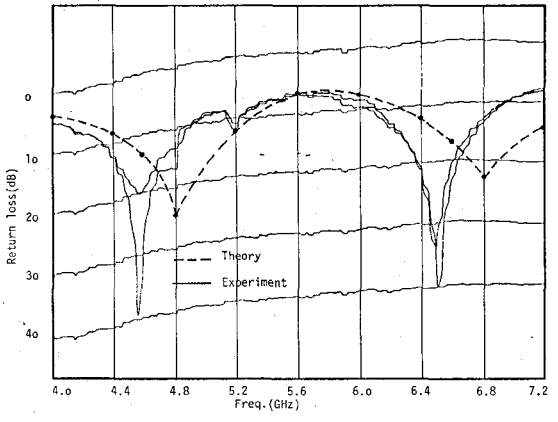

Fig. 4. Return loss versus frequency of two back-to-back microstrip to coplanar waveguide tapers (Fig. 2).

tion have been measured by 8410A-HP network analyzer over the frequency range of 4–7.2 GHz, and are shown in Fig. 4, together with the theoretical results. In principle, the two measurements should read the same values. But, in practice, due to asymmetry present in connecting the OSM connectors and difficulties in making the two tapers identical, the return losses are not equal from each termination. This fact is clearly seen in the given graph. Nonetheless, as is noticed from the same graph, except at those frequencies where the return losses are small and extraneous sources of reflections become conspicuous, the two measured return losses could be considered almost identical. Comparison of theory and experiment shown in Fig. 4, suggests that a good agreement exists between them, especially if a frequency shift of 0.3 GHz is permitted. The discrepency might be attributed to the deviation of the practical transition from its theoretical model.

IV. *X*-Band and *Ka*-Band Waveguide to Fin-Line Taper

Transferring electromagnetic energy from waveguide to all metal fin line, or to the dielectric supported fin line built in the body of the same waveguide, is often achieved by tapering the metallic ridges. Therefore a portion of

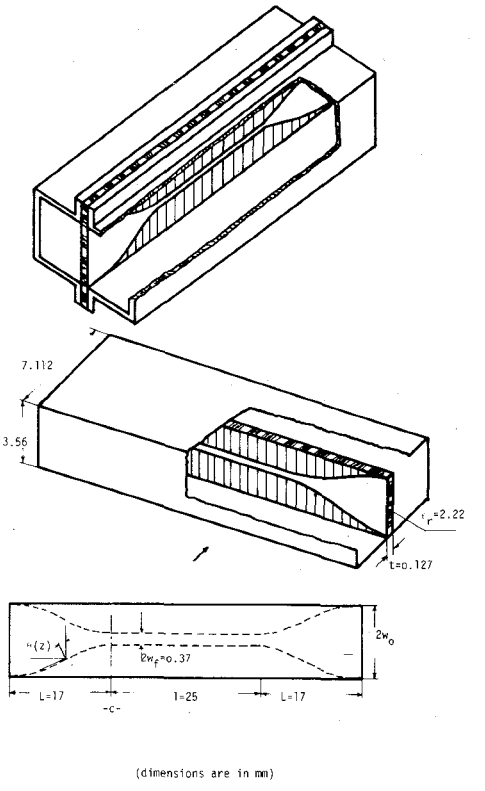

Fig. 5. *Ka*-band waveguide to fin line to waveguide transition.

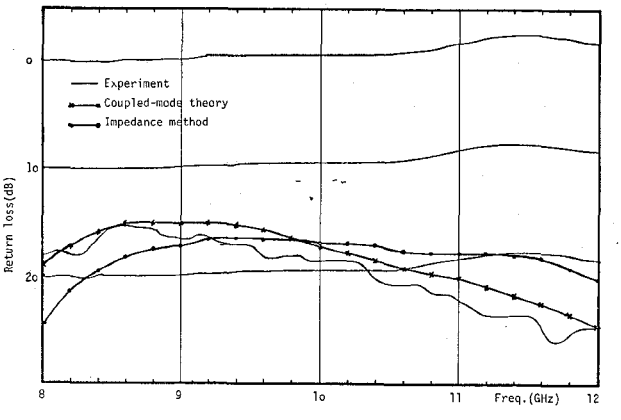

Fig. 6. Return loss versus frequency of the *X*-band transition.

incident energy being initially in TE_{10} mode is converted into finline mode [16]. Obviously the taper efficiency varies with its profile.

A very good matched-load is readily available for the rectangular waveguide; thus, for the purpose of accurate measurement, it is desirable to construct two waveguide to fin-line transitions positioned in opposite directions (Fig. 5). The gap profile for each taper is given by

$$w(z) = w_0 - (w_0 - w_f)\sin^2\frac{\pi z}{2L} \tag{24}$$

where w_0, w_f, and L are shown in Fig. 5. The above profile is chosen for convenience to ensure the smoothness of the taper.

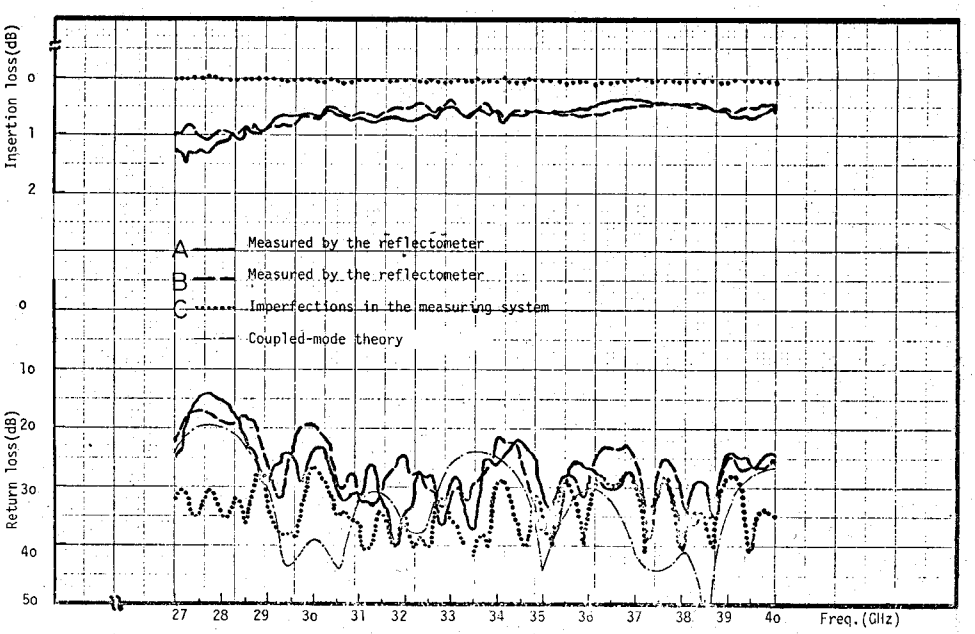

Fig. 7. Return loss versus frequency of the *Ka*-band transition. *A* and *B* denote measurements at different terminal planes.

With reference to Fig. 5 given for the *Ka*-band transition, the dimensions are chosen to be $L=25$ mm, $l=10$ mm, $w_f=1$ mm, and $t=0$. The theoretical and experimental values of return loss for this particular transition over *X*-band are shown in Fig. 6. It is apparent from this graph that the measurements are more consistent with the results derived by the developed field method, (12), than those given via the impedance approach, (13).

Very similar measurement and analysis as explained for the *X*-band transition, were carried out for the *Ka*-band back-to-back taper, Fig. 5. Results depicted in Fig. 7 reveal that this transition indeed reflects a small amount of incident power. Therefore, due to mismatches and imperfections present in the measuring instruments and in the fabrication process, an accurate comparison of theory and experiment is difficult. Nevertheless, at frequencies where the theoretical transition reflection is most significant, the effect of the mentioned extraneous sources of error is minimized and then theory and experiment seem consistent.

V. Conclusions

A class of MIC gradual planar transition has been formulated and successfully applied through the coupled-mode theory combined with the spectral domain approach. This combination gives the opportunity of fast and accurate computation of reflection coefficient. In some cases, such as a microstrip to coplanar-waveguide taper, or waveguide to fin-line taper, it was found that the computing times for this rigorous field technique and the simple impedance approach were almost equal. On the other hand, it was found that for some tapers, (e.g., where the dielectric cross section remains constant along the taper such as for a microstrip taper), the numerical evaluation of $C(z)$ requires more accurate field components than those provided by the zero order solution of the spectral domain technique, [5], [13]. The latter is adequate for $\rho(z)$, but values of $C(z)$ depend upon more careful numerical differentiation of (22).

The impedance technique (13) along with the coupled-mode method has also been studied in other transitions, [5]. It appears that this simple method is only valid at low frequencies for those tapers whose associated normal modes can be derived through a quasi-static solution. Since the presented method has been developed in a general form, only one computer program with some modification can be utilised for a broad class of transitions.

References

[1] W. Menzel, "Calculation of inhomogeneous microstrip lines," *Electron. Lett.*, vol. 13, pp. 183–184, Mar. 1977.
[2] S. A. Schelkunoff, "Generalised telegraphist's equations for waveguides," *Bell Syst. Tech. J.*, vol. 31, pp. 784–801, 1952.
[3] R. E. Collin, *Foundation for Microwave Engineering*. New York: McGraw-Hill, 1966.
[4] W. Getsinger, "Microstrip characteristic impedance," *IEEE Trans. Microwave Theory Tech.*, vol. MTT-27, p. 293, Apr. 1979.
[5] D. Mirshekar-Syahkal, "Analysis of uniform and tapered transmission lines for microwave integrated circuits," Ph.D. thesis, University of London, London, England, 1979.
[6] J. B. Davies and D. Mirshekar-Syahkal, "Spectral domain solution of arbitrary coplanar transmission lines with multilayer substrate," *IEEE Trans. Microwave Theory Tech.*, vol. MTT-25, pp. 143–146, 1977.
[7] V. V. Shevchenko, *Continuous Transitions in Open Waveguides*. Boulder, CO: Golem Press, 1971.
[8] A. F. Stevenson, "General theory of electromagnetic horns," *J. Appl. Phys.*, vol. 22, pp. 1447–1460, 1951.
[9] R. E. Collin, *Field Theory of Guided Waves*. New York: McGraw-Hill, 1960.
[10] A. W. Snyder, "Coupling of modes on a tapered dielectric cylinder," *IEEE Trans. Microwave Theory Tech.*, vol. MTT-18, pp. 383–392, 1970.
[11] S. S. Saad, "Computer analysis and design of gradually tapered waveguides with arbitrary cross-sections," Ph.D. thesis, University of London, London, England, 1973.
[12] L. Solymar, "Spurious mode generation in nonuniform

waveguides," *IRE Trans. Microwave Theory Tech.*, vol. MTT-7, pp. 379–383, 1959.
[13] D. Mirshekar-Syahkal and J. B. Davies, "Accurate solution of microstrip and coplanar structures for dispersion and for dielectric and conductor losses," *IEEE Trans. Microwave Theory Tech.*, vol. MTT-27, pp. 694–699, 1979.
[14] D. Mirshekar-Syahkal and J. B. Davies, "Computation of the shielded and coupled microstrip parameters in suspended and conventional form," *IEEE Trans. Microwave Theory Tech.*, vol. MTT-28, pp. 274–275, 1980.
[15] C. P. Wen, "Coplanar waveguide: A surface strip transmission line suitable for non-reciprocal gyromagnetic device applications," *IEEE Trans. Microwave Theory Tech.*, vol. MTT-17, pp. 1087–1090, 1969.
[16] G. Begemann, "An *X*-band balanced finline mixer," *IEEE Trans. Microwave Theory Tech.*, vol. MTT-26, pp. 1007–1011, Dec. 1978.

Maximum *Q*-Factor of Microstrip Resonators

ANAND GOPINATH, SENIOR MEMBER, IEEE

***Abstract*—The quality factors of microstrip half-wavelength resonators have been calculated as a function of substrate thickness, for frequencies in the range 8–96 GHz, for different ϵ_r. Conductor, dielectric, and radiation losses have been included. The optimum substrate thickness for the maximum *Q*-factor for 50-Ω microstrip resonators has been derived as a function of frequency for different dielectric constants.**

I. Introduction

MICROSTRIP is used as the guiding and interconnecting structure in microwave integrated circuit modules up to 100 GHz. While microstrip conductor and dielectric dissipation may be expressed as loss per unit length, radiation losses may only be related to specific lengths of line. The quality factors of resonators, which include radiation losses, thus provide a guide to the losses that occur in microstrip. The *Q*-factors of half-wavelength resonators have been calculated as functions of substrate thickness and frequency, for some commonly used dielectric material. Belohoubek and Denlinger [1] have previously reported *Q*-factor calculations for $\lambda/4$ resonators using Pucel, Masse, and Hartwig's method [2] for conductor loss and Lewin's method [3] for radiation loss, over a limited frequency range. Our calculations show good agreement with their results for the 8-GHz case.

From these results, the optimum substrate thickness for maximum *Q*-factors of half-wavelength resonators may be obtained for a given frequency. In cases where radiation losses and spurious coupling problems exist, these calculations provide a guide to the optimum substrate thickness. When packaging eliminates these effects, the thickness is limited by the spurious mode excitation in the structure. Choice of substrate thickness may also be determined by thermal conductance, circuit, and processing considerations as well as material availability.

Manuscript received July 14, 1980; revised September 24, 1980. This work was sponsored by the Department of the Army. The views and conclusions contained in this document are those of the contractor and should not be interpreted as necessarily representing the official policies, either expressed or implied, of the United States Government.

The author is with M.I.T. Lincoln Laboratory, Lexington, MA.

II. Theoretical Considerations

The stored energy U, in a $\lambda_g/2$ resonator with a voltage distribution of $V\sin\beta_g z$ is given by

$$U=\frac{V^2}{8Z_0 f} \tag{1}$$

where Z_0 is the resonator impedance and f is the frequency. The conductor and dielectric losses W_l in the resonator are given by

$$W_l=\frac{1}{4}\frac{V^2}{Z_0}\lambda_g(\alpha_d+\alpha_c) \tag{2}$$

where α_c and α_d are the conductor and dielectric loss constants in nepers per unit length. Thus the circuit quality factor Q_0 is given by

$$Q_0=\frac{2\pi fU}{W_l}=\frac{\pi}{\lambda_g(\alpha_c+\alpha_d)}. \tag{3}$$

The radiation Q is estimated by calculating the total power radiated W_r and evaluating the ratio

$$Q_r=\frac{2\pi fU}{W_r}. \tag{4}$$

The total quality factor Q_t is given by

$$\frac{1}{Q_t}=\frac{1}{Q_0}+\frac{1}{Q_r}. \tag{5}$$

The conductor loss constant α_c is estimated from the expression [2]

$$\alpha_c=\frac{R_s}{2Z_0 I^2}\left[\int_{-w/2}^{+w/2}J_s^2\,dx+\int_{-\infty}^{+\infty}J_{gp}^2\,dx\right] \tag{6}$$

where

J_s strip current;
J_{gp} ground plane current;
I total strip or ground plane current;

0018-9480/81/0200-0128$00.75 ©1981 IEEE